

The Luminescence of Some Oxidic Bismuth and Lead Compounds

C. W. M. TIMMERMANS AND G. BLASSE

Solid State Department, Physics Laboratory, Utrecht University, P.O. Box 80.000, 3508 TA Utrecht, The Netherlands

Received August 19, 1983; in revised form December 9, 1983

The luminescence properties of the bismuth compounds $\text{Bi}_2\text{Ge}_3\text{O}_9$, $\text{Bi}_{12}\text{MO}_{20}$ ($M = \text{Ge}, \text{Ti}$), and $\text{Bi}_2\text{Al}_4\text{O}_9$ and of the lead compounds PbGe_3O_7 and PbM_2O_4 ($M = \text{Al}, \text{Ga}$) are reported and discussed. $\text{Bi}_{12}\text{MO}_{20}$ and probably PbGe_3O_7 show semiconductor-type luminescence. For $\text{Bi}_{12}\text{MO}_{20}$ blue and red emission bands are reported which both are ascribed to radiative recombination at (deep) defect centre levels in the band gap. The blue emission originates probably from surface defects. The other compounds show broad emission and excitation bands with large Stokes shifts. The transitions occur on one and the same Bi^{3+} (Pb^{2+}) ion. From decay time measurements it is found that the energy difference between the two lowest excited levels is very small for all compounds. The large Stokes shifts and small trap depths are discussed in terms of the asymmetrical coordination of the $6s^2$ ions in the compounds under discussion. It is concluded that asymmetrically surrounded Bi^{3+} ions give rise to luminescence which is characterized by a broad emission band which shows a very large Stokes shift (≈ 2 eV).

1. Introduction

Since the 1930's many investigators have been concerned with the optical properties of the mercury-like ions Tl^+ , Pb^{2+} , and Bi^{3+} (e.g., 1-5). The absorption spectra of these ions consist of the so-called *A*, *B*, and *C* bands in order of increasing energy. They are ascribed to transitions from the 1S_0 ($^1A_{1g}$) ground state to the 3P_1 ($^3T_{1u}$), 3P_2 ($^3E_u + ^3T_{2u}$), and 1P_1 ($^1T_{1u}$) excited states, respectively (1). Low-lying C.T. transitions from the ligands to the $6s^2$ ion can give rise to *D* band absorption (2). The emission of these ions originates at low temperatures from the 3P_0 ($^1A_{1u}$) state, the transition being strongly forbidden. At higher temperatures the emission occurs mainly from the 3P_1 level, which transition is allowed by spin-orbit mixing of the 3P_1 and 1P_1 states.

Our laboratory has also been engaged in the investigations of the luminescence of these ions, especially of Pb^{2+} (6, 7) and Bi^{3+} (8-10) as a dopant in several (mainly oxidic) host lattices.

The positions of the emission and excitation bands of the bismuth ion depend strongly on the composition of the host lattice. In some compounds the emission is found in the ultraviolet region; other compounds exhibit visible luminescence up to the red spectral region. Compounds with small Stokes shifts usually produce spectra with vibrational structure (5, 9, 10), whereas compounds with a large Stokes shift show broad band emission (3, 4). The energy difference between the 3P_0 and 3P_1 levels frequently seems to be related to the value of the Stokes shift (11).

The site symmetry of the $6s^2$ ion may in-

fluence the optical properties. From the structural data of bismuth compounds it is known that the $6s^2$ ions prefer an asymmetric coordination, with short oxygen bonds on one side and others with longer bond distances on the other side (see, e.g., Ref. (12)). This asymmetric coordination is ascribed to the presence of the $6s^2$ lone pair, which points in the direction of the longer-bonded oxygen atoms. As an example we mention $\text{Bi}_4\text{Ge}_3\text{O}_{12}$ (Ref. (14)), in the crystal structure of which the Bi^{3+} ion has three oxygen atoms at 2.16 Å on one side, and three others at 2.60 Å on the other side. The site symmetry is C_{3v} . On the other hand, if the $6s^2$ ion occupies a small (octahedral) hole in a host lattice, it probably occupies the central metal position because of lack of space. Unfortunately it is very difficult to determine by direct means the exact site symmetry of $6s^2$ ions in a host lattice. Therefore we decided to investigate a number of oxidic bismuth and lead compounds in which the $6s^2$ ions are known to be coordinated asymmetrically. In Table I these compounds and some structural data are summarized. In the compounds $\text{Bi}_2\text{Ge}_3\text{O}_9$ and $\text{Bi}_4\text{Ge}_3\text{O}_{12}$ the Bi^{3+} ion exhibits C_{3v} site

symmetry, and in $\text{Bi}_2\text{Al}_4\text{O}_9$ approximately, if one considers the long Bi–O bonds as less important. The other compounds have lower site symmetry for the s^2 ions.

Also, energy migration through the lattice could occur in these compounds, since the shortest Bi–Bi and Pb–Pb distances amount to about 4 Å. These short interatomic distances could produce considerable wave function overlap, leading to semiconductor-type luminescence; i.e., the excitation into the band gap yields free charge carriers, giving rise to photoconductivity. This has been reported for $\text{Bi}_{12}\text{GeO}_{20}$ (20). It is interesting to ascertain whether PbGe_3O_7 , which has even shorter Pb–Pb distances, also exhibits this behavior. Although we observed semiconductor-type luminescence in some cases, we were nevertheless able to demonstrate that asymmetrically surrounded $6s^2$ ions produce a characteristic type of luminescence.

2. Experimental

2.1. Sample Preparation

The measurements on $\text{Bi}_2\text{Ge}_3\text{O}_9$ and

TABLE I
STRUCTURAL DATA OF SOME BISMUTH AND LEAD COMPOUNDS

	$\text{Bi}_2\text{Ge}_3\text{O}_9$	$\text{Bi}_4\text{Ge}_3\text{O}_{12}$	$\text{Bi}_{12}\text{GeO}_{20}$ $\text{Bi}_{12}\text{TiO}_{20}$	$\text{Bi}_2\text{Al}_4\text{O}_9$ $\text{Bi}_2\text{Ga}_4\text{O}_9$	PbGe_3O_7	PbAl_2O_4 PbGa_2O_4
Reference	13	14	15, 16	17	18	19
Approximate site symmetry of the $6s^2$ ion	C_{3v}	C_{3v}	C_{1h}	C_{3v}	C_1	C_{1h}
Coordination	6	6	7	6	7	6
Bond lengths (Å)	2.14 (3×) 2.74 (3×)	2.16 (3×) 2.60 (3×)	2.07 2.22 (2×) 2.63 (2×) 3.08 3.17	2.11 2.18 (3×) 2.41 2.91 (2×)	2.36 2.43 2.48 2.62 (2×) 2.87 2.99	2.26 2.40 (2×) 2.80 3.25 (2×)
Shortest $6s^2$ – $6s^2$ ion distance (Å)	4.0	4.5	3.6	4.1	3.4	4.3

PbGe_3O_7 were performed on crystals which were kindly put at our disposal by the authors of Refs. (13, 18), viz. Dr. B. C. Grabmayer of Siemens Laboratories in München, and Dr. H. H. Otto of the University of Regensburg, respectively.

Powders of $\text{Bi}_{12}\text{GeO}_{20}$ and $\text{Bi}_{12}\text{TiO}_{20}$ were prepared by firing Bi_2O_3 and GeO_2 or TiO_2 in an oxygen atmosphere at a temperature of 850°C for 5 h. A small amount of excess Bi_2O_3 was used to compensate for losses by evaporation. In the case of $\text{Bi}_{12}\text{GeO}_{20}$, 1% BiF_3 was added to accelerate the reaction. Powders of $\text{Bi}_2\text{Al}_4\text{O}_9$ were prepared from a NaCl flux containing Bi_2O_3 and Al_2O_3 . Powders of PbAl_2O_4 and PbGa_2O_4 were prepared by dissolving the oxides in nitric acid, evaporating the solution, and firing the nitrates in an oxygen atmosphere at 700°C for 10 hr. All samples were checked by X-ray powder diffraction.

2.2 Instrumentation

The luminescence and decay time measurements were performed on an apparatus described in Ref. (9). The decay times of the lead compounds were determined using a photo-counting system (EG&G) (see Fig. 1). The optical part is conventional. The excitation source consists of a pulsed Xe, N_2 , or D_2 flash lamp. The excitation wavelength is selected by means of band pass filters.

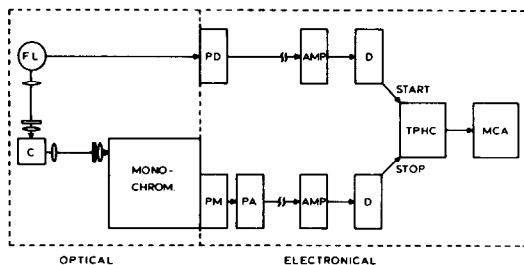


FIG. 1. Schematic representation of the photon counting system used for decay time measurements. FL, flash lamp; C, cryostat; PD, photodiode; PM, photomultiplier; PA = preamplifier; D, discriminator; TPHC, time-to-pulse height converter; MCA, multi-channel analyzer; and AMP, amplifier.

The emission wavelength is selected by a double monochromator (Jobin Yvon, HRD1). The central feature of the electronical part is the time-to-pulse height converter (TPHC), which converts the time interval between a certain start and stop pulse into a pulse with a corresponding amplitude. These pulses are analyzed by a multichannel analyzer (MCA). The start pulses are generated directly from the lamp flash by a photodiode (PD). The stop pulse is generated by a photon entering the photomultiplier tube (RCA C31034).

3. Results

3.1. Bismuth Compounds

3.1.1. Bismuth germanates. The results of the luminescence measurements on $\text{Bi}_2\text{Ge}_3\text{O}_9$ have been reported elsewhere (21). The luminescence of $\text{Bi}_4\text{Ge}_3\text{O}_{12}$ has been described in the literature (22, 23). For semiconducting $\text{Bi}_{12}\text{GeO}_{20}$ the luminescence properties at 80 K have also been reported (24). Here we add luminescence measurements on $\text{Bi}_{12}\text{GeO}_{20}$ at liquid-helium temperature. The emission and excitation spectra of the luminescence of these three compounds at 4.2 K are presented in Fig. 2. The temperature dependence of the emission intensity and of the decay time of the three compounds are given in Fig. 3.

(i) $\text{Bi}_2\text{Ge}_3\text{O}_9$. The emission spectrum of $\text{Bi}_2\text{Ge}_3\text{O}_9$ consists of one Gaussian band peaking at 2.4 eV for band edge excitation at 4.9 eV (see Fig. 2a). Another emission band, peaking at 2.3 eV, was encountered upon excitation at 3.85 eV (21). The decay time of the 2.4 eV emission at low temperatures is about 70 μsec and decreases above 5 K to a level of about 10 μsec (see Fig. 3a). The emission intensity is constant up to about 80 K at which temperature thermal quenching of the luminescence sets in. No photoconductivity was observed upon excitation into the optical band gap (21).

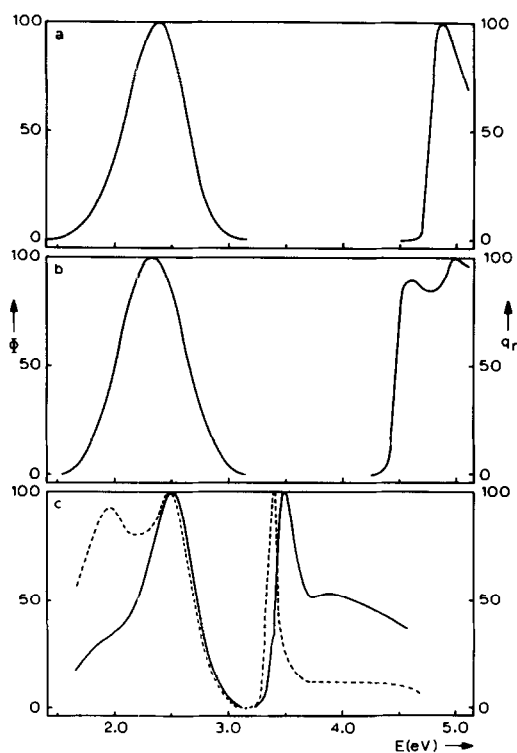


FIG. 2. Emission and excitation spectra of the luminescence of (a) $\text{Bi}_2\text{Ge}_3\text{O}_9$, (b) $\text{Bi}_4\text{Ge}_3\text{O}_{12}$, and (c) $\text{Bi}_{12}\text{GeO}_{20}$ at 4.2 K. For $\text{Bi}_{12}\text{GeO}_{20}$ the emission spectra were recorded upon 3.4 eV (---) and 3.5 eV (—) excitation and the excitation spectra for $E_{em} = 1.9$ eV (---) and $E_{em} = 2.5$ eV (—). Here and in other figures Φ denotes the photon flux per constant energy interval in arbitrary units and q_r the relative quantum output.

(ii) $\text{Bi}_4\text{Ge}_3\text{O}_{12}$. The luminescence properties of $\text{Bi}_4\text{Ge}_3\text{O}_{12}$ are similar to those of $\text{Bi}_2\text{Ge}_3\text{O}_9$. The emission band is situated at 2.35 eV if excitation takes place at energies ≥ 4.6 eV (Fig. 2b, after Ref. (23)). No defect luminescence such as found for $\text{Bi}_2\text{Ge}_3\text{O}_9$ has been reported. Also, the temperature dependences of the decay times of both compounds exhibits a similar behavior (see Fig. 3b, after Ref. (23)). The luminescence intensity, however, quenches at much higher temperatures than in the case of $\text{Bi}_2\text{Ge}_3\text{O}_9$.

(iii) $\text{Bi}_{12}\text{GeO}_{20}$. In Ref. (4) a red emission band is reported for $\text{Bi}_{12}\text{GeO}_{20}$ at 80 K with

a maximum at 1.95 eV. At 4.2 K we observed in addition a blue emission band peaking at 2.5 eV. The excitation spectra of the two emission bands are somewhat different. The blue emission has a strong excitation peak at 3.5 eV, with a shoulder at 3.4 eV, while for the red emission the excitation maximum is at 3.4 eV. The broad excitation band at higher energies is less intense for the 1.9 eV emission than for the 2.5 eV emission (Fig. 2c). Excitation at energies ≥ 3.5 eV does not lead to red emission, not even at temperatures where the blue luminescence is quenched. The broad excitation band measured for 1.9 eV emission must therefore be due to the blue emission, which has a tail stretching down to that emission energy.

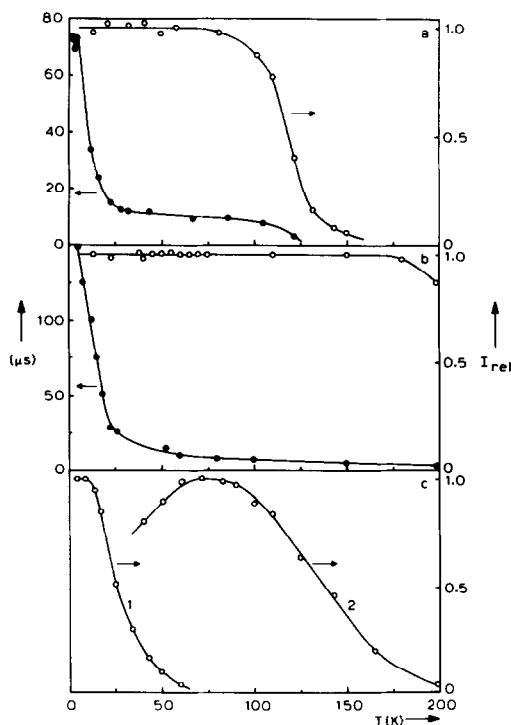


FIG. 3. Emission intensity (○) and decay time (●) as a function of temperature for the emissions of (a) $\text{Bi}_2\text{Ge}_3\text{O}_9$, (b) $\text{Bi}_4\text{Ge}_3\text{O}_{12}$, and (c) $\text{Bi}_{12}\text{GeO}_{20}$ (curve 1: blue emission under 3.4 and 3.5 eV excitation; curve 2: red emission under 3.4 eV excitation).

In Fig. 3c the intensity of the blue emission band is given as a function of temperature (curve 1). The thermal quenching already starts at 15 K. Above 60 K no blue luminescence is observable. The intensity of the red emission increases in the quenching region of the blue emission upon excitation at 3.4 eV (curve 2). The red luminescence quenches at temperatures higher than 80 K, in agreement with Ref. (24). The decay curves of both emissions are exponential. The decay times at 4.2 K are short, viz. 8 μsec for the blue emission and approximately 5 μsec for the red one. No long decay times could be observed. The decay time of the red luminescence does not change much upon raising the temperature. According to Ref. (24) the decay time is still 3 μsec at 80 K, where thermal quenching sets in.

3.1.2. Bismuth Titanate. The compound $\text{Bi}_{12}\text{TiO}_{20}$ shows the same emission and excitation spectra as $\text{Bi}_{12}\text{GeO}_{20}$, although the peak positions are somewhat shifted. For $\text{Bi}_{12}\text{TiO}_{20}$ they are 1.9 and 2.6 eV for the red and blue emission bands, respectively. The excitation maxima are situated at 3.35 eV for the red emission band and at 3.4 eV for the blue one. Also the temperature dependences of the emission intensities exhibit the same behavior, although the red luminescence quenches at lower temperatures than in the case of $\text{Bi}_{12}\text{GeO}_{20}$.

3.1.3. Bismuth Aluminate. In Refs. (25,

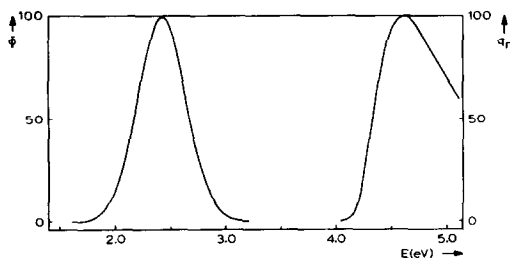


FIG. 4. Emission and excitation spectra of the luminescence of $\text{Bi}_2\text{Al}_4\text{O}_9$ at 4.2 K.

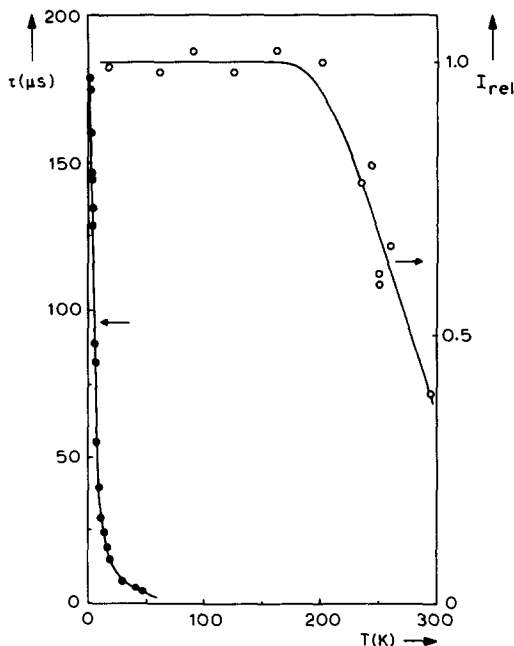


FIG. 5. Emission intensity (O) and decay time (●) of the luminescence of $\text{Bi}_2\text{Al}_4\text{O}_9$ as a function of temperature. The excitation energy was 4.6 eV.

26) a blue luminescence is reported for $\text{Bi}_2\text{Al}_4\text{O}_9$ which is still present at room temperature. Figure 4 shows the emission and excitation spectra of $\text{Bi}_2\text{Al}_4\text{O}_9$ at 4.2 K. The emission spectrum consists of a band peaking at 2.4 eV. The excitation spectrum consists of a band with a maximum at 4.6 eV. Upon excitation at 3.3 eV a broad red emission band is observed at about 1.9 eV. The compound $\text{Bi}_2\text{Ga}_4\text{O}_9$ produces similar spectra (26).

In Fig. 5 the temperature dependences of the decay time and of the intensity of the blue emission are shown. Bismuth aluminate exhibits a fairly strong luminescence at room temperature. The thermal quenching of the luminescence starts at about 200 K. At 1.3 K the decay time is rather long, viz. 180 μsec , but it decreases very steeply when the temperature is raised. From this curve a trap depth can be estimated which is only 1.5 meV.

3.2. Lead Compounds

3.2.1. Lead germanate. The emission spectrum of PbGe_3O_7 consists of a broad emission band which can be resolved into two Gaussian bands with maxima at 2.1 and 2.7 eV. The excitation spectrum is the same for both emission bands, viz. a band peaking at 3.75 eV (see Fig. 6a). Both emission bands quench in the same thermal region (see Fig. 7). We were not able to measure the decay curves of the two emissions separately because they overlap considerably and have the same excitation band. At liquid-helium temperature the decay curve of the total emission can be described by two exponential functions with decay times of about 10 and 70 μsec .

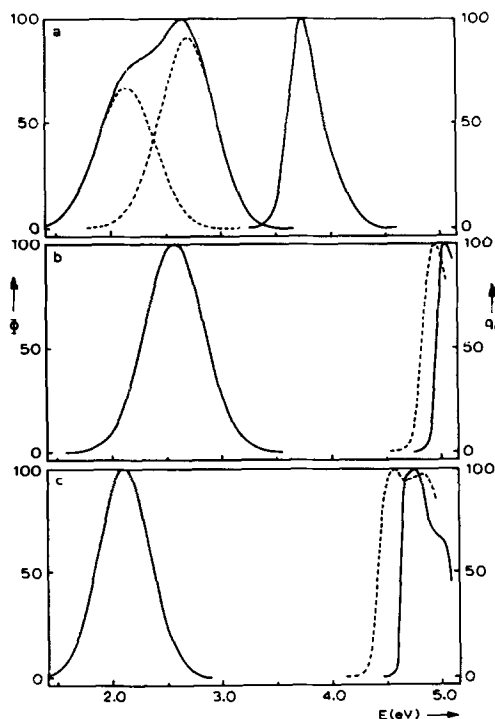


FIG. 6. Emission and excitation spectra of the luminescence of (a) PbGe_3O_7 , (b) PbAl_2O_4 , and (c) PbGa_2O_4 . For PbGe_3O_7 the emission band is resolved into two Gaussian bands. The excitation spectra of PbAl_2O_4 and PbGa_2O_4 are given at 4.2 K (solid line) and at room temperature (dashed line). Emission spectra were recorded at 4.2 K.

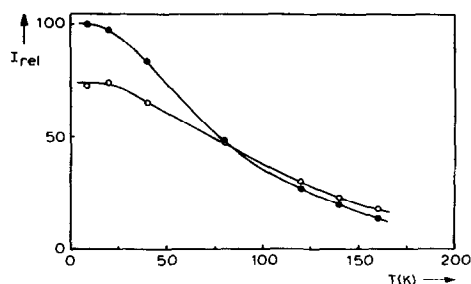


FIG. 7. Emission intensity of the 2.15 eV (O) and the 2.7 eV (●) emission bands of PbGe_3O_7 as a function of temperature. The excitation energy was 3.75 eV.

3.2.2. Lead aluminate and lead gallate. The compounds PbAl_2O_4 and PbGa_2O_4 produce strong blue and yellow luminescence, respectively at room temperature. At 4.2 K the emission spectra consist of broad bands peaking at 2.6 eV for PbAl_2O_4 and at 2.1 eV for PbGa_2O_4 (Figs. 6b and c). The shapes and positions of the emission bands do not change much upon heating up to room temperature. At low temperatures the excitation bands are situated at 5 eV for PbAl_2O_4 and at 4.7 eV for PbGa_2O_4 .

Figure 8 shows the thermal behavior of the luminescence intensities and of the decay times of PbAl_2O_4 and PbGa_2O_4 . The thermal quenching of the luminescence of lead gallate starts at approximately 200 K, while the emission intensity of PbAl_2O_4 is constant up to room temperature. All decay curves are exponential. Up to 60 K, the decay times are constant, approximately 70 μsec for PbGa_2O_4 and 65 μsec for PbAl_2O_4 . Above 60 K both emissions become faster with a thermal activation energy of about 70 meV.

The results of the investigations of the luminescence of these compounds are summarized in Table II.

4. Discussion

4.1. The Nature of the Optical Transitions

From the literature it is known that Bi_{12}

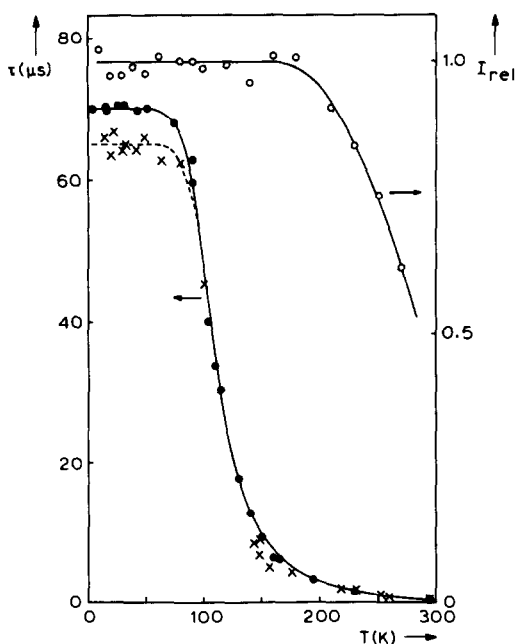


Fig. 8. Emission intensity (O) and decay time (●, x) as a function of temperature of PbGa_2O_4 (O, ●) and PbAl_2O_4 (x), for optical band-edge excitation.

GeO_{20} exhibits photoconductivity upon band-gap excitation (20), so that free charge carriers are formed. A similar situation has been observed by us for $\text{Cs}_3\text{Bi}_2\text{Br}_9$ (27). The valence and the conduction band are built up from mainly 6s orbitals and 6p orbitals of bismuth, respectively. The excitation band at 3.4 eV (Fig. 2c) therefore corresponds to an interband transition. The emission spectrum of $\text{Bi}_{12}\text{GeO}_{20}$ is quite complex. In addition to the blue and red luminescence, emission bands have been reported at 1.1, 1.4, and 1.8 eV at 80 K (28). Since we are dealing with a semiconductor the emissions may all be due to radiative recombination at defects.

The transition at 3.4 eV is ascribed to the band-gap transition of $\text{Bi}_{12}\text{GeO}_{20}$. The blue emission can be excited via the band-gap transition, but also at energies exceeding the band gap. It is therefore concluded that the blue emission is due to luminescence of

defects which are concentrated at or near the surface. This explanation seems the more probable, since the samples used for our experiments were powders. Further experiments at low temperatures on single crystals of $\text{Bi}_{12}\text{GeO}_{20}$ are necessary to elucidate the nature of the luminescence centres in this compound.

The nature of the optical transitions of the three other bismuth compounds, viz. $\text{Bi}_2\text{Ge}_3\text{O}_9$, $\text{Bi}_4\text{Ge}_3\text{O}_{12}$, and $\text{Bi}_2\text{M}_4\text{O}_9$ ($M = \text{Al}, \text{Ga}$) is more localized. The luminescence spectra of these compounds are similar. They show a broad emission band with a maximum at about 2.4 eV and an excitation band which is situated at high energies. In spite of the large Stokes (>2 eV) shift these bismuth compounds show a strong luminescence up to high temperatures. This must be related to the high energy of the excited state (29). Obviously, $\text{Bi}_2\text{Ge}_3\text{O}_9$, with the largest Stokes shift (2.5 eV) quenches at the lowest temperature.

As has been argued elsewhere (21, 26, 30), energy transfer between Bi^{3+} ions can be excluded in these materials. From a physical point of view they can be compared with a luminescent material such as CaWO_4 (31), which produce quite similar spectra. Excitation into the Bi^{3+} ion of these compounds is followed by a strong relaxation, so that the Stokes shift is large and energy transfer, impossible.

TABLE II
LUMINESCENCE PROPERTIES OF SOME BISMUTH AND LEAD COMPOUNDS

	$E_{\text{max}}^{\text{ex}}$ (eV)	$E_{\text{max}}^{\text{em}}$ (eV)	Stokes shift (eV)	Trap depth (eV)	$T_{1/2}$ (K)
$\text{Bi}_2\text{Ge}_3\text{O}_9$	4.9	2.4	2.5	0.002	120
$\text{Bi}_4\text{Ge}_3\text{O}_{12}$	4.6	2.35	2.25	0.003	270
$\text{Bi}_{12}\text{GeO}_{20}$	3.5, 3.4	2.5, 1.95	1.0, 1.45		25, 140
$\text{Bi}_{12}\text{TiO}_{20}$	3.4, 3.35	2.6, 1.9	0.8, 1.45		20, 80
$\text{Bi}_2\text{Al}_4\text{O}_9$	4.6	2.4	2.2	0.002	280
PbGe_3O_9	3.75	2.7, 2.15	1.05, 1.6		80, 100
PbAl_2O_4	5.0	2.6	2.4	0.075	>300
PbGa_2O_4	4.7	2.1	2.6	0.069	290

It is striking that the sillenites $\text{Bi}_{12}\text{MO}_{20}$ ($M = \text{Si}, \text{Ge}, \text{Ti}$) show an absorption edge more than 1 eV lower in energy than the other bismuth compounds under investigation (see, e.g., Fig. 2). A similar observation is made by comparing the semiconductor CsPbCl_3 and the insulator PbCl_2 (Ref. (30)). In the present model the lower absorption energy in the case of the semiconductor must be ascribed to broadening of energy levels into bands, whereas in the other compounds the excitation remains at a particular site, accompanied by a distortion of the surrounding lattice (self-trapped state) (32).

The luminescence spectra of the lead compounds PbAl_2O_4 and PbGa_2O_4 are comparable to those of the nonsemiconducting bismuth compounds. They show broad emission and excitation bands with a large Stokes shift. The excitation bands are shifted toward higher energies, as compared to the bismuth compounds, which is to be expected for lead-containing compounds. Probably as a consequence of the higher excitation energy, the luminescence of these compounds quenches at even higher temperatures than that of the corresponding bismuth compounds $\text{Bi}_2\text{Al}_4\text{O}_9$ and $\text{Bi}_2\text{Ga}_4\text{O}_9$ (26). The lower quenching temperature of PbGa_2O_4 in comparison with PbAl_2O_4 can be related to the larger Stokes shift and the lower excitation energy of the gallate.

The luminescence properties of PbAl_2O_4 and PbGa_2O_4 are similar to those of PbSO_4 which has the baryte structure with an irregular 12 coordination (33). In PbSO_4 the excitation maximum is even at approximately 5.5 eV and the emission maximum, at 3.4 eV. For all three compounds we assign the absorption band to intrinsic Pb^{2+} ions, which produce a considerably Stokes-shifted emission due to strong relaxation of the excited state.

The trap depths of the lead compounds are considerably larger (≈ 70 meV) than

those of the bismuth compounds under investigation (≈ 2 meV). A few examples of temperature-dependent lifetime measurements on lead centers are cited in the literature. For lead centres in cubic CaO and SrO a trap depth of about 100 meV was observed (34). On the other hand, $\text{CaZrO}_3\text{-Pb}^{2+}$ has a trap depth of about 10 meV (35). For a discussion on the trap depth, see below.

Finally we investigated the compound PbGe_3O_7 , which shows a much smaller Stokes shift than the other lead compounds. The optical bandgap is at much lower energies than for PbAl_2O_4 and PbGa_2O_4 (see Fig. 6). The shift of the excitation peak to lower energies can be explained by assuming that band formation prevails in PbGe_3O_7 . This is similar to the case of $\text{Bi}_{12}\text{GeO}_{20}$ mentioned above. One might argue that the low lead content in PbGe_3O_7 makes this explanation unlikely, but considerable wave function overlap between the lead ions is possible, since the lead ions in PbGe_3O_7 form chains with lead-lead distances of only 3.4 Å. The two emission bands are then due to radiative recombination at defect levels in the band gap. The interpretation that the 3.75 eV excitation band of PbGe_3O_7 corresponds to band gap excitation requires confirmation by photoconductivity measurements. Unfortunately available the crystals were not large enough to perform such an experiment.

4.2. The Effect of the Asymmetric Coordination of the $6s^2$ Ions on the Optical Properties

4.2.1. *The Stokes shift.* The compounds which we have investigated exhibit off-center positions for Bi^{3+} and Pb^{2+} which amount to a shift of 10–12% (see Table I). The asymmetric coordination of these ions is due to the presence of the lone pair, which is situated at the side opposite to the shorter bonded ions. In terms of wave functions and for the case of C_{3v} site symmetry,

the lone pair can be regarded as a linear combination of the $6s$ and $6p_z$ A.O.'s on the $6s^2$ ion. The $6p_x$ and $6p_y$ A.O.'s do not mix with $6s$ under C_{3v} symmetry and remain degenerate (see Fig. 9). This result agrees with that from a HFS (Hartree-Fock-Slater) calculation on BiX_3 ($X = \text{Cl, Br, I}$) molecules by Egdell *et al.* (36). These molecules also have C_{3v} symmetry. A transition from the asymmetric ground state $2a_1$ to the first excited state $2e$ results in a more symmetric coordination, i.e., the $6s^2$ ion moves from an off-center position to a position which is closer to the centre of the coordination polyhedron. The shift of the equilibrium position upon excitation yields a large Stokes shift, as is well known from the configurational-coordinate diagram. This is a simple method for representing the large relaxation of the excited state in these compounds.

The general conclusion from this reasoning is that Bi^{3+} ions on off-center positions are characterized by broad emission bands with large Stokes shifts. This section shows the general validity of this conclusion by presenting results for many compounds of $6s^2$ ions of which the crystal structure is accurately known and the asymmetric coordination is therefore proven.

On the other hand, a small Stokes shift and/or vibrational structure has only been observed for $6s^2$ ions on small (often octahedral) sites. We consider both types of Bi^{3+} luminescence as characteristic extremes. This suggests that the strong varia-

tion of the Stokes shift in Bi^{3+} -activated phosphors (11) is due to a certain off-center positioning of the Bi^{3+} ion. This point is under study in our laboratory.

4.2.2. *The trap depth.* In Ref. (11) it was noticed that the energy difference between the 3P_0 and 3P_1 states, the trap depth, seems to be related to the Stokes shift. A small trap depth is associated with a large Stokes shift and vice versa. Earlier it was shown that the large relaxation of the excited state of s^2 ions originates from an off-center to center shift upon excitation of the s^2 ions. This connects the relaxation to the site symmetry of the s^2 ions in the ground state. In this way it seems not unlikely that one can correlate the smaller trap depth with the lower site symmetry of the s^2 ions.

Since the trap depth reveals the level splitting of the excited state of the s^2 ion, we tried to obtain simple energy level diagrams. In the literature this is usually done by Russel-Saunders (LS) coupling. In view of the strong spin-orbit coupling in the case of $6s^2$ ions we considered *jj*-coupling as well. In Table III we present the results for the free ion and for C_{3v} site symmetry (as a typical example of a $6s^2$ ion in asymmetrical coordination). For LS-coupling the A.O.'s of Fig. 9 have been used, for *jj*-coupling the following one-electron orbitals were considered: free ion $6s_{1/2} < 6p_{1/2} < 6p_{3/2}$; for C_{3v} symmetry $e_{1/2} < e_{1/2} < e_{3/2} < e_{1/2}$ (after Ref. (36)). Note that the final splitting of the lowest excited state is due to (weak) spin-orbit interaction in the case of LS-coupling and to (weak) electron-electron interaction in the case of *jj*-coupling.

For the free ion case in the LS-coupling scheme the trap depth is $E(^3P_1 - ^3P_0)$, 3P_0 being the lower level. This holds also for cubic symmetry. For the *jj*-coupling scheme it is hard to predict the sequence of the levels which appear due to electron-electron interaction. For the free ion as well as for C_{3v} symmetry we have a level which can act as a trap level (3P_0 and A_2 , respectively).

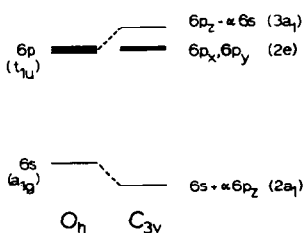


FIG. 9. Atomic orbitals of the Bi^{3+} ion for cubic and trigonal coordination.

TABLE III
ENERGY LEVELS INVOLVED IN s^2 LUMINESCENCE (SEE TEXT)

Coupling scheme	Site symmetry	Ground state	Lowest excited state ^a
LS	Free ion	$6s^2 \rightarrow {}^1S_0$	$6s6p \rightarrow {}^3P \rightarrow P_0 + \underline{P_1} + P_2$
LS	C_{3v}	$(2a_1)^2 \rightarrow {}^1A_1$	$2a_12e \rightarrow {}^3E \rightarrow \underline{A_1} + \underline{A_2} + \underline{2E}$
<i>jj</i>	Free ion	$(6s_{1/2})^2 \rightarrow S_0$	$6s_{1/2}6p_{1/2} \rightarrow \underline{P_0} + \underline{P_1}$
<i>jj</i>	C_{3v}	$(e_{1/2})^2 \rightarrow A_1$	$e_{1/2}e_{1/2} \rightarrow \underline{A_1} + \underline{A_2} + \underline{E}$

^a Transitions between the ground state and the lowest excited state are only allowed for the underlined levels.

Since the $6s^2$ ions are probably situated somewhere between the LS- and *jj*-coupling schemes, it is hard to predict the level structure of the excited state. It is clear, however, that small as well as large trap depths are possible. The absence of a trap level also is a possibility. This has been observed recently for KBr-Pb²⁺ by Schmitt *et al.* (37) and for some luminescent Bi³⁺ centers by Wolfert *et al.* (38). It should also be realized that a three-level scheme may be insufficient to explain the decay time results when the symmetry is lower than cubic.

These arguments show that the temperature dependence of the decay time of the luminescence of a $6s^2$ ion can vary from compound to compound, in good agreement with observations in this section and with the literature. The exact nature of the relation between trap depth and Stokes shift remains unclear, although a lower crystal field will certainly contribute to a decrease of the trap depth due to the resulting level splitting.

4.3. Concluding Remarks

This paper shows that asymmetrically coordinated $6s^2$ ions give rise to luminescence which is characterized by broad bands which are strongly Stokes shifted. This observation may present the key to understand the structure sensitivity of the Bi³⁺ emission in oxides. An exact determination

of the level structure of the excited state appears difficult within the present theoretical framework. Part of the proposals made in this section need to be confirmed by photoconductivity and luminescence measurements on single crystals at low temperatures.

Acknowledgments

The authors are indebted to Mr. O Boen Ho for his assistance in the experiments and to Professor E. J. Baerends and Dr. J. G. Snijders (Free University, Amsterdam) for an instructive discussion on the energy levels of the Bi³⁺ ion. The investigations were carried out as part of the research program of the Stichting voor Fundamenteel Onderzoek der Materie (FOM) and with financial support from the Nederlandse Organisatie voor Zuiver Wetenschappelijk Onderzoek (ZWO).

References

1. F. SEITZ, *J. Chem. Phys.* **6**, 150 (1938).
2. T. TSUBOI, *Phys. Rev. B* **22**, 4972 (1980).
3. G. BLASSE AND A. BRIL, *J. Chem. Phys.* **48**, 217 (1968).
4. G. BOULON, *J. Phys.* **32**, 333 (1971).
5. A. E. HUGHES AND G. P. PELLIS, *Phys. Status Solidi B* **71**, 707 (1975).
6. A. J. H. EYKELENKAMP, *J. Lumin.* **15**, 217 (1977).
7. J. A. GROENINK AND G. BLASSE, *J. Solid State Chem.* **32**, 9 (1980).
8. A. C. VAN DER STEEN, J. J. A. VAN HESTEREN, A. ROOS, AND G. BLASSE, *J. Lumin.* **18/19**, 235 (1979).
9. A. C. VAN DE STEEN, J. J. A. VAN HESTEREN, AND A. P. SLOK, *J. Electrochem. Soc.* **128**, 1327 (1981).

10. A. C. VAN DER STEEN, *Phys. Status Solidi B* **100**, 603 (1980).
11. G. BLASSE AND A. C. VAN DER STEEN, *Solid State Commun.* **31**, 993 (1979).
12. A. F. WELLS, "Structural Inorganic Chemistry," 4th ed., p. 712, Oxford Univ Press (Clarendon), Oxford (1975).
13. B. C. GRABMAIER, S. HAUSSÜHL, AND P. KLÜFFERS, *Z. Kristallogr.* **149**, 261 (1979).
14. A. DURIF AND M. AVERBUCH-POUCHOT, *C.R. Acad. Sci. (Paris) II* **295**, 555 (1982).
15. S. C. ABRAHAMS, P. B. JAMIESON, AND J. L. BERNSTEIN, *J. Chem. Phys.* **47**, 4034 (1967).
16. SH. M. EFENDIEV, T. Z. KULIEVA, V. A. LOMONOV, M. I. CHIRAGOV, M. GANDOLFO, AND P. VECCHIA, *Phys. Status Solidi A* **74**, K17 (1981).
17. R. ARPE AND HK. MÜLLER-BUSCHBAUM, *J. Inorg. Nucl. Chem.* **39**, 233 (1977).
18. H. H. OTTO, *Z. Kristallogr.* **149**, 197 (1979).
19. K.-B. PLÖTZ AND H. K. MÜLLER-BUSCHBAUM, *Z. Anorg. Allg. Chem.* **488**, 38 (1982).
20. G. G. DOUBLAS AND R. N. ZITTER, *J. Appl. Phys.* **39**, 2133 (1967).
21. C. W. M. TIMMERMANS, O BOEN HO, AND G. BLASSE, *Solid State Commun.* **42**, 505 (1982).
22. M. J. WEBER AND R. R. MONCHAMP, *J. Appl. Phys.* **44**, 5495 (1973).
23. R. MONCORGÉ, B. JACQUIER, AND G. BOULON, *J. Lumin.* **14**, 337 (1976).
24. R. B. LAUER, *Appl. Phys. Lett.* **17**, 178 (1970).
25. L. A. BRIXNER, *Mater. Res. Bull.* **13**, 563 (1978).
26. G. BLASSE AND O BOEN HO, *J. Lumin.* **21**, 165 (1980).
27. C. W. M. TIMMERMANS AND G. BLASSE, *Phys. Status Solidi B* **106**, 647 (1981).
28. V. A. GUSEV AND A. P. ELISEEV, *Avtometriya* **5**, 47 (1981).
29. K. C. BLEYENBERG AND G. BLASSE, *J. Solid State Chem.* **28**, 303 (1979).
30. R. C. POWELL AND G. BLASSE, *Struct. Bonding* **42**, 43 (1980).
31. G. BLASSE, *Struct. Bonding* **42**, 1 (1980).
32. Y. TOYOZAWA, *J. Lumin.* **12/13**, 13 (1976).
33. G. BLASSE, *Chem. Phys. Lett.* **35**, 299 (1975).
34. A. C. VAN DER STEEN AND L. T. F. DYCKS, *Phys. Status Solidi B* **104**, 283 (1981).
35. A. W. M. BRAAM AND G. BLASSE, *Solid State Commun.* **20**, 717 (1976).
36. R. G. EGDELL, M. HOTAKKA, L. LAAKSONEN, P. PYYKKÖ, AND J. G. SNIJDERS, *Chem. Phys.* **72**, 237 (1982).
37. K. SCHMITT, V. S. SIVASANKAR, AND P. W. M. JACOBS, *J. Phys. C: Solid State Phys.* **16**, 615 (1983); *J. Lumin.* **27**, 313 (1982).
38. A. WOLFERT AND G. BLASSE, *Mater. Res. Bull.*, in press.